Chemistry & Biology
Article

Application of Chemoproteomics to Drug Discovery: Identification of a Clinical Candidate Targeting Hsp90

Patrick Fadden,[1] Kenneth H. Huang,[1] James M. Veal,[1,*] Paul M. Steed,[1] Amy F. Barabasz,[1] Briana Foley,[1] Mei Hu,[1] Jeffrey M. Partridge,[1] John Rice,[1] Anisa Scott,[1] Laura G. Dubois,[1] Tiffany A. Freed,[1] Melanie A. Rehder Silinski,[1] Thomas E. Barta,[1] Philip F. Hughes,[1] Andy Ommen,[1] Wei Ma,[1] Emilie D. Smith,[1] Angela Woodward Spangenberg,[1] Jeron Eaves,[1] Gunnar J. Hanson,[1] Lindsay Hinkley,[1] Matthew Jenks,[1] Meredith Lewis,[1] James Otto,[1] Gijsbertus J. Pronk,[1] Katleen Verleysen,[1] Timothy A. Haystead,[2] and Steven E. Hall[1]
[1]Serenex, Inc., 323 Foster Street, Durham, NC 27701, USA
[2]Department of Pharmacology and Cancer Biology, Duke University Medical Center, Durham, NC 27710, USA
*Correspondence: jveal@pamlicopharma.com
DOI 10.1016/j.chembiol.2010.04.015

SUMMARY

A chemoproteomics-based drug discovery strategy is presented that utilizes a highly parallel screening platform, encompassing more than 1000 targets, with a focused chemical library *prior* to target selection. This chemoproteomics-based process enables a data-driven selection of both the biological target and chemical hit after the screen is complete. The methodology has been exemplified for the purine binding proteome (proteins utilizing ATP, NAD, FAD). Screening of an 8000 member library yielded over 1500 unique protein-ligand interactions, which included novel hits for the oncology target Hsp90. The approach, which also provides broad target selectivity information, was used to drive the identification of a potent and orally active Hsp90 inhibitor, SNX-5422, which is currently in phase 1 clinical studies.

INTRODUCTION

The discovery of new medicines continues to challenge the pharmaceutical industry (GAO Report, 2006). A central issue is that the identification of new drug candidates via pharmaceutical research is an extended linear effort. Although modern technological improvements have accelerated segments of the drug discovery process, this linear pathway to discovery has remained largely unchanged: target identification, biological assay development, primary screening to identify chemical hits, hit-to-lead exploration, lead optimization, secondary or selectivity screening, and finally candidate selection.

Chemoproteomics-based screening approaches, directed at molecules which target purine binding proteins, have been shown recently to be able to provide substantial binding information with regards to both targets inhibited and relative binding affinities. (Graves et al., 2002; Haystead, 2006; Duncan et al., 2008). In particular, these methods utilize Sepharose resins coupled with electrophoresis and mass spectrometry to evaluate noncovalent binding interactions. Since both selectivity and affinity information is obtained in a single experiment, parallelization of two steps of the drug discovery process (primary and secondary screening) is achieved. Selectivity information is of significant value for the purine-binding proteome given that it has many druggable targets but also a number of proteins whose functional inhibition would be expected to be detrimental. The purine proteome consists of ~1500 proteins as defined by an ability to utilize a purine cofactor, such as ATP, NAD, or FAD (Uniprot, 2008).

We report here further development and extension of this chemoproteomics-based approach. In particular, we apply it a direct manner to drug discovery by utilizing it in conjunction with a focused chemical library. Of significance is that the library screening is done prior to target selection, and thus the drug discovery steps of target identification, primary screening, and secondary screening are conducted in parallel across multiple targets. We describe the design and application of the methodology to the chaperone protein Hsp90 which is currently an oncology target of high interest (Banerji, 2009). This effort has led to the discovery of SNX-5422 as a highly selective, orally active Hsp90 inhibitor for oncology that is in phase 1 clinical trials.

RESULTS

Screening Results

The first step in the approach used here was creation of a suitable chemical library. A 5000 member focused compound library was designed from commercially available compounds with the goal of creating a maximally diverse compound set that was targeted for any purine cofactor site across the proteome. Cheminformatic approaches (see Experimental Procedures; see Supplemental Experimental Procedures available online) were used to develop and refine descriptors that allowed preferential identification of known purine protein binding compounds from a pool of several million compounds. The computed fingerprints incorporated general features of the molecule (e.g., number hydrogen bond donors and acceptors, number of rings) as well as specific topological torsions and finally the presence or absence of characteristic purine binding motifs. These descriptors were then used to select uncharacterized compounds for screening. The

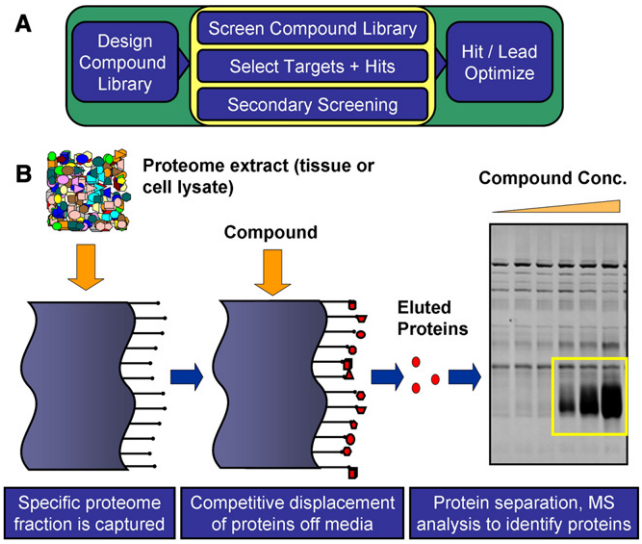

Figure 1. Overview of Chemoproteomics-Based Discovery Process

(A) Schematic indicating that steps that are typically sequential in drug discovery (yellow oval) are now accomplished in parallel fashion through use of the screening methodology.

(B) Schematic of screening technique which is initiated by loading of a proteome extract onto an optimized affinity chromatography resin. Subsequent challenge with a compound will compete off the resin proteins with sufficient binding affinity for that compound and these proteins can be identified via mass spectrometry techniques.

Table 1. Summary Results from Chemical Library Screen

Target Affinity Screen Results			
Library	Unique Compound-Protein ID's	Unique Compounds	Unique Proteins
Initial (5000)	963	463	77
Follow-up (3000)	616	185	81
Total (8000)	1579	648	118
Cellular Assay Results			
Library	IC_{50} <1 μM	IC_{50} <5 μM	IC_{50} <10 μM
Initial (5000)	38	96	117
Follow-up (3000)	70	171	295
Total (8,000)	108	267	412

Target Affinity Screen Results	
Protein Family	Members Eluted
Actin/myosin related	5
ATP binding ligase	6
Chaperone	7
Metabolic kinase	12
Serine/threonine kinase	22
Receptor tyrosine kinase	15
Nonreceptor tyrosine kinase	8
NAD oxidoreductase	17
Other miscellaneous classes	26
Total	118

library was profiled against the purine-binding proteins from porcine lung or liver, evaluating each compound at a single concentration with follow-up screening of selected compounds at three concentrations as illustrated in Figure 1.

The breadth of the screening method was demonstrated by the identification of proteins from a wide variety of enzyme families, including both ATP-binding and NAD-binding enzymes. Gene families represented included hydrolases, kinases, dehydrogenases, tranferases, carboxlyases, and chaperone proteins. From the initial library of 5000 compounds, approximately 1000 unique compound-protein pairs were identified, which comprised 463 compounds, eluting a total of 77 distinct proteins (Table 1). Initial structure-activity relationships of the hits were explored through the acquisition of a 3000 member follow-up library that was selected based on chemical similarity to the initial 463 hits. This latter library was screened in the same manner generating about 600 compound-protein pairs (comparable hit rate to the initial library). Of the 85 proteins eluted by the 185 follow-up compounds, 41 of the proteins were new and had not been observed in the screen of the first 5000 member collection. An additional effort was aimed at identifying, at an early stage, compound-target interactions which might also demonstrate cellular effects. In parallel, the library compounds were screened for their ability to inhibit proliferation in three cell lines (MCF-7, NCI-H460, HUVEC), with a total of about 250 compounds displaying IC_{50} values of less than 5 μM.

Examples of the raw data generated from an unbiased screen are illustrated in Figure 2. In Figure 2A, three compounds (**1**–**3**) from distinct structural classes are compared for the proteins they eluted. Compounds **1** and **2** were examples of compounds eluting a single target, pyridoxal kinase (PDXK) and 3-hydroxyacyl-CoA dehydrogenase (HCDH), respectively, with clean binding profiles otherwise. Conversely, compound **3** clearly showed a dual inhibition profile to proteins Hsp90 and S-adenosylhomocysteine hydrolase (SAHH).

These examples were also selected to illustrate the range of proteins that can be profiled. PDXK, HCDH, Hsp90, and SAHH are from distinct protein families with diverse functions (Uniprot, 2008): PDXK is essential to vitamin B6 synthesis; HCDH is an enzyme of beta fatty acid oxidation, and SAHH is involved in methylation function and homocysteine metabolism. Additionally, Hsp90 and PDXK utilize ATP whereas HCDH and SAHH use NADH as a cofactor (Uniprot, 2008). Despite the inherent complexity of screening hundreds of protein targets in parallel, the method is also sufficiently sensitive to highlight target selectivity differences between closely related compounds as shown in Figure 2B. For example, purine **4** eluted alcohol dehydrogenase (ADH4) as well as modestly eluting Hsp90 family member endoplasmin (GRP94) while minimal binding to Hsp90 isoforms alpha and beta was observed. In contrast, the close analog **5** showed enhanced Hsp90 elution, diminished GRP94 elution, and did not elute ADH4 but instead showed interaction with SAHH. Quite remarkable is the difference observed between two very closely related analogs of methotrexate; t-butyl analog **7** shows significant affinity for 2,4-dienoyl reductase (DECR) whereas the olefin analog **6** does not elute this target but displays a higher affinity for pyruvate carboxylase (PYC) and propionyl CoA-carboxylase (PCCA, PCCB). More generally, methotrexate and a range of analogs were found to show appreciable binding (IC_{50}'s <150 nM, data not shown) to biotin carboxylase

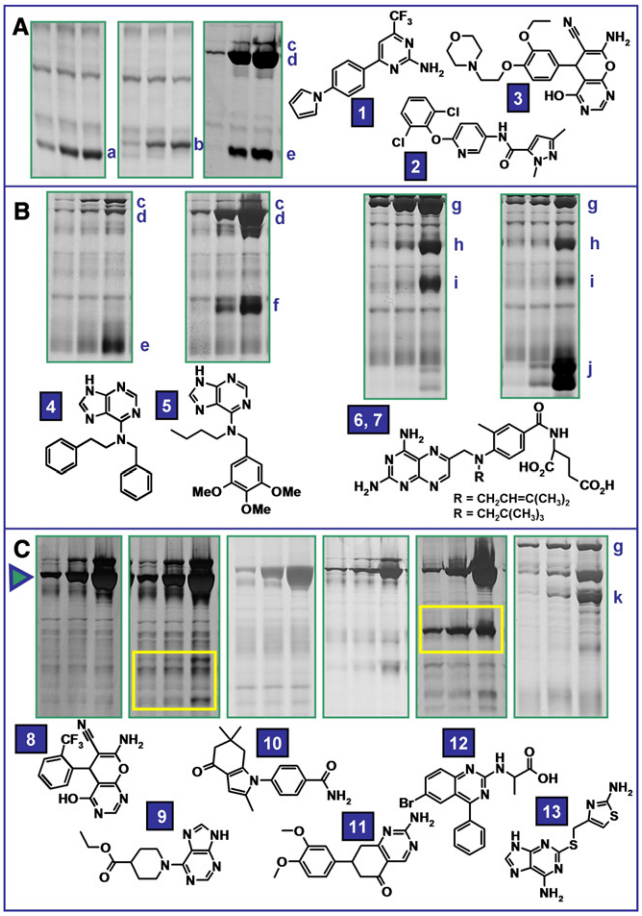

Figure 2. Screening a Targeted Library

For all gels, compound concentrations increase from left to right (20, 50, and 500 μM). Protein identifications: a = PDXK; b = HCDH; c = GRP94; d = HSP90 (α and β); e = SAHH; f = ADH4; g = PYC; h = PCCA; i = PCCB; j = DECR; k = synapsin.

(A) Protein elution profiles of individual compounds from porcine lung. Compounds **1** and **2** are representative of compounds that eluted one primary target whereas compound 3 illustrates a dual inhibitor identified in the screening process.

(B) Protein elution profiles of two closely related pairs of compounds from porcine liver. Despite a high degree of similarity, compounds display a distinct target elution profile.

(C) Example compounds that eluted Hsp90 (filled triangle) from affinity resin. Yellow boxes indicate off-targets, which were a series of protein kinases for compound **9** and ALDH2 for compound **12**.

family members PYC, PCCA, and PCCB at levels of potential therapeutic relevance.

Novel Hits for Hsp90

Of the compound-protein interactions identified in the initial screen, several involved the chaperone protein Hsp90. Hsp90 has emerged as a promising drug target in as well as other diseases involving mutant, foreign, or aberrantly expressed proteins oncology (Whitesell and Lindquist, 2005; Chiosis et al., 2004; Calderwood et al., 2006; Neckers, 2007; Solit and Chiosis, 2008). The client proteins of Hsp90 include a wide range of potentially oncogenic proteins, including Her2, c-Kit, and mutated EGFR. Hsp90 is an ATPase and this activity is required for it to maintain the proper folding of its client proteins (Obermann et al., 1998; Panaretou et al., 1998; Pearl and Prodromou, 2006; Pratt and Toft, 2003). Early work on inhibitors of Hsp90 focused on natural product ansamycins and radicicol (Whitesell et al., 1994; Sharma et al., 1998; Schulte et al., 1998; Stebbins et al., 1997; Roe et al., 1999), as well as small molecule purine and resorcinol-based scaffolds (Janin, 2005; Chiosis and Tao, 2006; Powers and Workman, 2007; Kasibhatla et al., 2007; Brough et al., 2008; Dymock et al., 2005; Vilenchik et al., 2004). At the time of the screen, geldanamycin analogs, 17-AAG and 17-DMAG, had entered early clinical development; however, due to a general lack of oral bioavailability of 17-AAG, as well as potential for chemical reactivity, identification of novel small molecule inhibitors of Hsp90 would be highly desirable.

The initial hits for Hsp90 identified by this screen possessed structural novelty and diversity. Several hits are shown in Figure 2C; only one of the six compounds shown, compound **13**, contained an adenine substructure. The data for Hsp90 further illustrated the capability of the approach to provide secondary screening information in addition and parallel to that generated for the primary target of interest. In particular, purine **9** and quinazoline **12** both showed alternate protein elutions in addition to Hsp90 with **9** eluting a series of protein kinases and **12** demonstrating moderate affinity interactions with aldehyde dehydrogenase (ALDH2). Additional proteome mining using porcine brain tissue also revealed that compound **13** was observed to elute the protein Synapsin which regulates neurotransmitter release and has been shown to have an ATP binding domain (Esser et al., 1998). It would likely be highly undesirable to have off-target binding to this protein, and early identification of this interaction helped inform the decision to not pursue optimization of this particular scaffold. The ability of a focused library of small size to still provide a breadth of distinct scaffolds was demonstrated in that, subsequent to this work, publications and patent applications have appeared that describe compounds inhibiting Hsp90 that are closely related to, or in some cases identical to, compounds **8**, **9**, **11**, and **12** (Eggenweiler and Wolf, 2006; Carrez et al., 2006; Machajewski et al., 2006; Eggenweiler et al., 2006). This affinity-based screen also provided a unique advantage for the chaperone family; all four isoforms of Hsp90, Hsp90α, Hsp90β, Grp94, and Trap1, could be screened in a single assay.

Confirmation of ATP-Competitive Binding Mode

Based on both the combined attractiveness of Hsp90 as a target for oncology and the chemical hits emerging from the screen, Hsp90 was selected as a discovery program. In particular, benzamide **10** was selected for optimization based on its novelty, chemical tractability, and high degree of target selectivity. Medicinal chemistry exploration of amide **10** led to a number of initial analogs with increased affinity for Hsp90 while maintaining a high degree of selectivity. Implicit in the screening methodology, targeted at purine binding proteins, was the assumption that protein-compound interactions identified were due to competitive binding at the nucleotide binding site. Prior to more extensive optimization efforts, X-ray

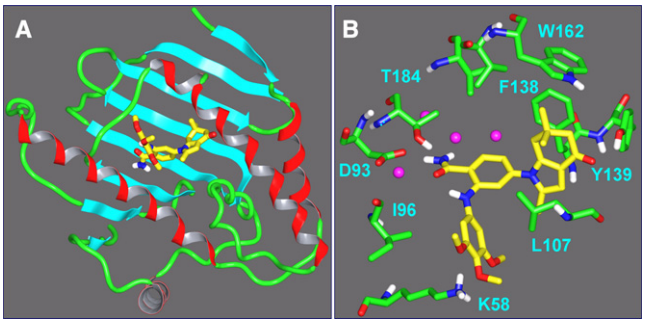

Figure 3. X-ray structure of Cocrystal of HSP90α with Benzamide Derivative 14, 2-(3,4,5-Trimethoxy-Phenylamino)-4-(2,6,6-Trimethyl-4-Oxo-4,5,6,7-Tetrahydro-Indol-1-yl)-Benzamide

(A) Ribbon view of the entire crystallized N-terminal domain (residues 1–232) with compound.

(B) Close-up view of the ATP binding site region of cocrystal showing binding mode of compound **14**. Key direct and indirect hydrogen bonds to Asp93, Thr184, and structural waters (magenta) mirror those observed in the crystal structure reported for ADP and ATP. Indolone binding site is formed by displacement of Leu107 from position occupied in ADP/ATP structures.

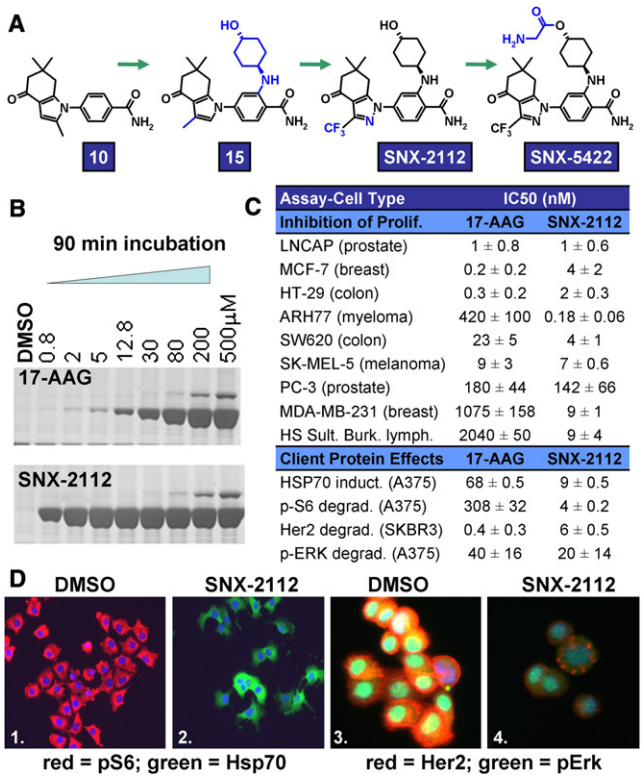

Assay-Cell Type	IC50 (nM)	
Inhibition of Prolif.	17-AAG	SNX-2112
LNCAP (prostate)	1 ± 0.8	1 ± 0.6
MCF-7 (breast)	0.2 ± 0.2	4 ± 2
HT-29 (colon)	0.3 ± 0.2	2 ± 0.3
ARH77 (myeloma)	420 ± 100	0.18 ± 0.06
SW620 (colon)	23 ± 5	4 ± 1
SK-MEL-5 (melanoma)	9 ± 3	7 ± 0.6
PC-3 (prostate)	180 ± 44	142 ± 66
MDA-MB-231 (breast)	1075 ± 158	9 ± 1
HS Sult. Burk. lymph.	2040 ± 50	9 ± 4
Client Protein Effects	**17-AAG**	**SNX-2112**
HSP70 induct. (A375)	68 ± 0.5	9 ± 0.5
p-S6 degrad. (A375)	308 ± 32	4 ± 0.2
Her2 degrad. (SKBR3)	0.4 ± 0.3	6 ± 0.5
p-ERK degrad. (A375)	40 ± 16	20 ± 14

Figure 4. Identification and In Vitro Pharmacology of SNX-2112

(A) Modifications of benzamide **10** leading to SNX-2112 and SNX-5422. Progressive changes to the chemical structures are indicated in blue.

(B) Concentration dependent elution of Hsp90 with a 90 min incubation of either 17-AAG or SNX-2112 and the protein-laden affinity resin. The IC_{50} for SNX-2112 determined by this approach is 30 nM.

(C) IC_{50} values for SNX-2112 and 17-AAG in tumor cell proliferation and Hsp90 client assays in nanomolars.

(D) High content screens were used to evaluate effects following SNX-2112 treatment. Panels 1 and 2 are images of A375 cells and show loss of pS6 (red) and induction of Hsp70 (green) following 1 μM SNX-2112 treatment. Panels 3 and 4 are images of AU565 cells and show loss of Her2 (red) and pERK (green) following 10 μM treatment with SNX-2112. Images of pS6/Hsp70 are 10x magnification collected using a Cellomics ArrayScan; a Becton Dickinson Pathway 435 instrument was used to collect the Her2/pERK images at 20× magnification.

crystallography was used to both experimentally validate this assumption and provide insights into strategies for optimization. An N-terminal domain construct (residues 1-232) of Hsp90α was readily cocrystallized with a derivative **14**, 2-(3,4,5-trimethoxy-phenylamino)-4-(2,6,6-trimethyl-4-oxo-4,5,6,7-tetrahydro-indol-1-yl)-benzamide, to yield a high quality structure with a maximum resolution of 1.9 Å (Figure 3A). The structure of the complex clearly demonstrated that binding to Hsp90 was targeted to the ATP binding site (Obermann et al., 1998; Panaretou et al., 1998; Prodromou et al., 1997), and this result confirmed the validity of the purine proteome-based screening strategy. In particular, the benzamide moiety provided analogous interactions to those observed for ATP or ADP with the amide oxygen and NH2 group mimicking adenine N1 and N6, respectively, by forming both direct and water mediated hydrogen bonds to Thr184 and Asp93 (Figure 3B). Additional hydrogen bonding and hydrophobic interactions were observed between the trimethoxy phenyl ring of compound **14** and Hsp90 residues Lys58, Met98, and Leu107. The ketone oxygen of the indolone ring also exhibited a well-formed hydrogen bond with the hydroxyl of Tyr139. In addition to this hydrogen bond, multiple favorable hydrophobic interactions were observed especially between the gem-dimethyl-cyclohexanone moiety of **14** and a series of hydrophobic residues (Met98, Leu103, Leu107, Phe138, Val150, and Trp162). The binding site for this moiety was largely formed by a conformational rearrangement that leads to Leu107 being displaced from its position occupied when ATP is bound. A similar rearrangement has been reported for purine-based inhibitors (Wright et al., 2004; Immormino et al., 2006). Met98 and Leu107 also pack tightly against the benzamide and trimethoxy phenyl components of compound **14**.

Identification of a Clinical Candidate, SNX-5422

Despite the richness in chemical diversity, none of the initial Hsp90 hits displayed activity in cell-based assays, regardless of whether antiproliferative activity or direct client protein effects were examined. However, the opportunistic pursuit of the readily tractable benzamide hit **10** allowed rapid progress as summarized in Figure 4. Assisted by structural information, design efforts led to compound **15** which showed potent binding to Hsp90 and cellular activity. Modifications to eliminate the potential metabolic liability at the C2 position of the pyrrole moiety of **15** in turn gave rise to SNX-2112 which displayed strong in vitro antiproliferative activity. SNX-2112 blocked the proliferation of all human tumor cells tested with IC_{50} values ranging from 0.2 to 140 nM (Figure 4C). Importantly, this compound exhibited comparable potencies in cell-based assays for client protein effects to those observed for antiproliferative endpoints. SNX-2112 induced well-established Hsp90 client protein effects, such as loss of Her2, abrogation of Akt and ERK signaling pathways (measured via pS6 and pERK levels), and induction of Hsp70 levels with EC_{50} values ranging from 3 to 9 nM (Figures 4C and 4D). In addition, the potency of SNX-2112 exceeded

that of 17-AAG in the vast majority of cell lines evaluated. The time-dependent increase in affinity reported for 17-AAG (Gooljarsingh et al., 2006) was similarly observed for SNX-2112. When evaluated using the purine-affinity media (Figure 4B), an increase in incubation time (from 5 to 90 min) of SNX-2112 produced a 10-fold increase in apparent affinity; calculated apparent Ki values for SNX-2112 binding were 22 and 1.5 nM, respectively.

In order to improve kinetic solubility of the crystalline form of SNX-2112, a glycine ester prodrug functionality was added, yielding SNX-5422 (Figure 4A). Conversion of ester SNX-5422 to parent SNX-2112 was rapid and complete in vivo following oral dosing (Figure 5A) and resulted in excellent exposure of the parent compound. Parameters calculated (WinNonlin software) for a single 30 mg/kg dose in female rats (n = 3) were $T_{1/2}$ = 6.0 hr; Tmax = 2 hr; Cmax = 2427 ng/ml; $AUC_{0\text{-inf}}$ = 19,232 hr*ng/ml; apparent volume of distribution = 13,600 ml/kg; apparent clearance = 1560 ml/hr/kg. SNX-5422 also displayed significant antitumor activity in various human tumor xenograft models in mice and, unlike other Hsp90 natural product inhibitors and their analogs, was highly effective when dosed orally. As illustrated in Figure 5B, administration (p.o. three times per week) SNX-5422 to nude mice implanted with BT-474 xenograft tumors resulted in regression of tumor growth. It is noteworthy that only nine doses of SNX-5422, administered over the first 3 weeks resulted in six of nine mice being tumor free after 6 months. No overt adverse effects related to compound were observed for the mice in the experiment. Coadministration of SNX-5422 (low dose) with the Her2 antibody, trastuzumab (Vogel et al., 2002), also resulted in tumor regression.

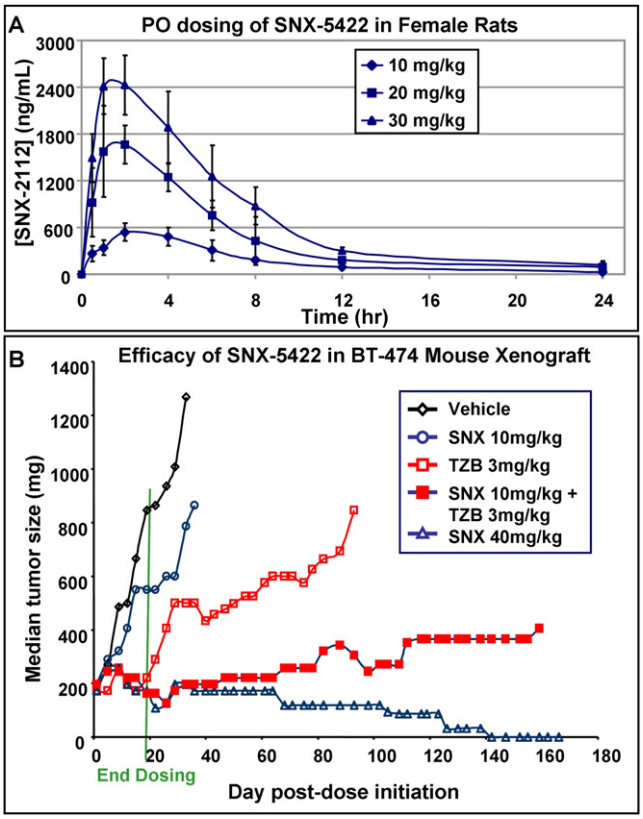

Figure 5. In Vivo Pharmacology of SNX-5422

(A) EXPOSURE of SNX-2112 following oral dosing of SNX-5422 in female rats. Data are from average of three animals with SEM shown. Levels of prodrug were below the lower limit of quantitation (LLOQ) at all time points.

(B) Effects on BT-474 tumor-bearing nude mice (n = 10) dosed with vehicle or (1) 10 mg/kg SNX-5422 (SNX) p.o. three times per week, (2) trastuzumab (TZB) 3 mg/kg i.v., two times per week, (3) 10 mg/kg SNX p.o. three times per week and TZB 3 mg/kg i.v., two times per week, or (4) 40 mg/kg SNX three times per week. Dosing in all drug-treated groups was for only the first 3 weeks. All groups were followed for 6 months or until sacrifice due to tumor burden.

DISCUSSION

The central step of the discovery methodology presented here is a chemoproteomics-based screening process that can be viewed as an extensively parallel competitive binding assay. The affinity media (Hardeman et al., 2004) was optimized to bind not only ATP-binding proteins, such as kinases, but also proteins that utilize other purine cofactors such as NAD. Binding of the proteins to the affinity resin is a fully reversible equilibrium process and involves no covalent modification (Figure 1). Additionally, it can be performed in a standard 96-well format where each well is challenged with a discreet compound. Both of these factors make the approach favorable for incorporation within a drug discovery framework. Specific tissues or cell types may be evaluated and compared for binding to a compound. In fact, typically a background gel pattern, characteristic of the specific tissue or cell type expressed proteome, is observed owing to the fact that binding of proteins to the resin is dynamic and reversible. Since the eluant, excluding background, is composed of only the proteins that possess affinity for the test compound, the eluant profile is often quite simple. However, the MS methods used are capable of identifying multiple proteins in the same gel band, with a practical limit of about four to five proteins per band. Compounds that are selective ligands may only elute a single protein where as promiscuous compounds, e.g., staurosporine, may elute dozens of targets from the affinity matrix.

Several important distinctions between this approach and traditional drug discovery are evident. First, the primary target need not be selected in advance of the screen since each compound is able to bind to any of the protein targets from the tissue. In this sense, the process is one of self-selection since the target is not selected without concomitant identification of a hit compound. If a given compound is evaluated at multiple concentrations, typically three concentrations in screening mode, binding affinity data can be ascertained. Additionally, broad target selectivity information is generated on each compound as a necessary consequence of the screen design. More informed follow-up of screening hits is thus enabled since the method provides not only the affinity of the compounds for a potential target of interest but also for a broad array of possible off-targets. Use of this screening approach throughout hit-to-lead and lead optimization provided ongoing target selectivity information to guide medicinal chemistry efforts. Finally, native protein is used for the screen, thereby obviating the often time-consuming steps of cloning, expressing, and purifying the protein in quantities sufficient for high-throughput screens.

The approach does not remove the need for ultimate target validation. In the case study provided here, Hsp90 was clearly already of interest in the scientific community with substantial validation that preceded the work. Additionally, X-ray crystallography, as described, was used to confirm the expected binding mode to Hsp90, and this step too will always remain in the discovery process. Nonetheless, there is no reason that the approach could not be applied to a previously uncharacterized biological target protein, and, as noted above, the advantages of immediately having both a tool compound and information on the selectivity profile of the compound would in principle facilitate validation of the target as one of interest.

The chemoproteomics approach utilized here can be compared to alternative approaches directed at the purine binding proteome. Use of reactive acyl phosphates has been shown to allow detection of at least 75% of protein kinases with good sensitivity to low abundance protein kinases (Patricelli et al., 2007). This approach can also be used in a compound screening mode. However, it differs from the method described here in that a given compound must be determined to block labeling of all proteins it inhibits within the context of the proteome (i.e., absence of signal) versus this approach where one is looking simply for a positive elution of proteins that are inhibited (i.e., generation of signal). Use of bead bound inhibitors as a chemoproteomics methodology has also been described (Bantscheff et al., 2007). Again this approach has been shown to have high sensitivity for detection and screening of compounds versus protein kinases. It is dependent on having known inhibitors to a target of interest and then using isobaric tags for mass spectrometry-based quantification. Although we have demonstrated the ability to detect a wide range of protein kinases, low-copy proteins are one of the challenges to this methodology, given that gel-based detection methods are employed. Its strengths are the ability to profile a wide range of purine binding protein family members with diverse protein folds, especially metabolic proteins, and be utilized in a true medium to high-throughput screening mode to evaluate chemical libraries.

Analysis of PFAM protein fold data (Finn et al., 2008) for the hits confirmed that the method can capture proteins from multiple protein fold families, including targets of interest for pharmaceutical intervention. For example, PDXK is a member of the pfkB ribokinase family containing several carbohydrate and pyrimidine kinases. Hsp90 is part of the HATPase_C group that includes gyrase, histidine kinase, and the mismatch repair protein mutL. PYC and PCCA/PCCB are both members of the biotin carboxylase family that also includes the fatty acid enzyme acetyl-CoA carboxylase which is currently metabolic drug target of some interest (Harwood, 2004). Finally, HCDH and SAHH fall into their own more distinct protein folds. SAHH has also received substantial interest as a drug target particularly with regards to its role in methylation and viral replication (Guillerm et al., 2006). Thus, the diversity of enzyme classes (Table 1), including both NAD and ATP binding proteins, and the range of protein families exemplified as detectable by the methodology support its ability to be utilized in a drug discovery mode for targets within the purine binding proteome capture.

This chemoproteomics approach has been exemplified via discovery of a clinical candidate targeting Hsp90. The screening methodology was used to identify compound-Hsp90 interactions, prior to Hsp90 being selected as a target. Hits were prioritized in terms of both binding affinity and selectivity through the methodology. In turn, these data facilitated rapid optimization of the preferred scaffold to cell active, orally bioavailable compounds. Based on its efficacy in multiple xenograft models, with a variety of oral dosing schedules, SNX-5422 was selected for clinical development and is currently in phase 1 trials in both solid and hematological tumor patients.

SIGNIFICANCE

The chemoproteomics approach described here provides a methodology by which a focused chemical library can be profiled against a broad set of relevant targets. The resulting data can then be analyzed to extract the best starting points, with respect to both biology and chemistry, for subsequent optimization. Because biological target choices are not made a priori in advance of screening, but rather based on the screening results, the mechanism is self-selecting. There are numerous improvements to still be made to the technology including improved sensitivity to low copy proteins, better handling of membrane proteins, and potential migration to non-gel-based methods. Extension of the method to other target classes, e.g., proteases and biogenic amine receptors, is also of interest. Nonetheless, proof of principle for the methodology has been demonstrated. In particular, the ability to provide parallelization to certain components of the discovery process has been shown with the result that a clinical candidate was rapidly derived from a small initial chemical library.

In conclusion, an unbiased affinity-based chemoproteomics screen was used to profile an 8000 member targeted library. This process self-selected Hsp90 as an attractive drug discovery target based on the novelty and selectivity of the screening hits. X-ray crystallography results confirmed that the proteome screen was functioning correctly. Optimization of one scaffold, using Hsp90-specific cell-based assays, led to the identification of SNX-2112 and SNX-5422 as orally active Hsp90 inhibitors. SNX-5422 is currently in phase 1 clinical trials in both solid and hematological tumor patients. This outcome validates the unique, high-content discovery process and represents a successful strategy toward the goal of increasing the efficiency of drug discovery.

EXPERIMENTAL PROCEDURES

Proteome Screening

The general approach involved preparing a tissue lysate that was then incubated with a purine-derived Sepharose affinity media (Hardeman et al., 2004; example 29). Porcine tissues (40 g) were homogenized in buffer A (120 ml) composed of 25 mM HEPES (pH 7.4), 60 mM NaCl, 20 mM $MgCl_2$, 30 mM Na-β-glycerophosphate, 1 mM DTT, 1 mM Na-vanadate, and a protease inhibitor cocktail. The homogenate was clarified by centrifugation at 100,000 ×g for 20 min and the resulting supernatant was decanted into a 6 ml slurry (1:1) of the Sepharose affinity media in buffer A. The affinity media was incubated with resin on ice for 45 min with gentle mixing. The proteome loaded affinity media was transferred to a gravity feed column and washed with 10 volumes of buffer A, followed by 20 volumes of buffer A plus 300 mM NaCl, and then 10 volumes of buffer B (25 mM HEPES [pH 7.4],

120 mM NaCl, 20 mM $MgCl_2$, 1 mM DTT, 1 mM Na-vanadate, and a protease inhibitor cocktail). The loaded resin was transferred in equal amounts to 96 well, 200 μl filtertip pipette tip columns. Incubation of the test compound with the protein-laden affinity matrix results in competitive binding for the protein targets. Compound challenge was performed on a Tecan TeMo liquid handler with compound in buffer B with 5% DMSO in a total volume of 75 ml. A compound with sufficient affinity for a given protein inhibits its binding to the affinity resin and the resulting compound-protein mixture was collected as the column eluant. The complexity of the eluted proteins was visualized following separation on a 1D SDS-PAGE gel with either Cypro ruby or silver staining. Proteins that were visualized above background were identified using standard trypsin gel band digest and MS/MS techniques (Rosenfeld et al., 1992; Gharahdaghi et al., 1999). Gel band isolation, trypsin protease digest, and mass spectrometry-based protein identifications were performed as described previously (Chandarlapaty et al., 2008) using Applied Biosystems/MDS SCIEX API 3000 or ABI 4700 MALDI TOF/TOF instrumentation. Apparent Ki values for SNX-2112 were calculated using the equation $Ki = IC_{50}/(1+[S]/Kd)$ where [S] = estimated purine resin concentration of 3 mM and the Kd for Hsp90 is taken as ~130 μM.

Focused Chemical Library Construction

The screening library was compiled from commercially available compound collections. Vendor files in SDF file format were obtained from 19 vendors and totaled approximately 2.4 million compounds. Algorithms (see below and Supplemental Experimental Procedures) were developed in house to profile each molecule based on its topology (bonds, dihedrals, rings, etc.) and other molecule related characteristics or descriptors such as the number of hydrogen bond donors and acceptors, hydrophobic moieties, and functional groups occurrences. Once topology and descriptor information had been generated, it was first used to filter molecules with undesirable properties such as reactive species, having too many occurrences of certain functional groups, or other general properties such as a high molecular weight. Eighty-five filters were used (see Supplemental Experimental Procedures) with the resulting elimination of approximately 50% of compounds.

The topology and descriptor information was then used to select compounds sufficiently like a target adenosine analog. Initially, 40 known purine target inhibitors (e.g., kinase inhibitors or methotrexate, see Supplemental Experimental Procedures) were profiled in the same manner as the compounds under consideration. The information was summarized algorithmically as a "fingerprint" array. Elements of the fingerprint were weighted such that when these test compounds were seeded into an otherwise random collection of compounds, and their (Sørensen, 1948) coefficients were calculated relative to deoxyadenosine plus one benzene (for additional hydrophobicity), they would be preferentially selected from the collection. The profiles of the compounds for purchase were then converted to fingerprints and weighted as with the test compounds. Again using Sørensen coefficients as similarity criteria, a set on the order of 150K molecules was selected. Clustering based on iterative maximal distance evaluation was then used to select ~10K compounds. Visual inspection by chemists reduced this set to the initial 5K screening library.

More specifically, the cheminformatic characterization of given molecule and similarity calculation between two molecules was as follows (see also Supplemental Experimental Procedures). Each atom was assigned a core functional type. For each regular or improper dihedral occurrence within a molecule, excluding those containing hydrogens, the atoms in that dihedral were converted to their functional types. Reference and test molecules were then compared for their overlap of dihedrals via a Sørensen-type calculation, and the calculated coefficient for this comparison was given a weighting factor of 33.3. Additionally, each molecule was profiled for the total number of occurrences of various features such as functional types, rings, and the presence or absence a purine binding motif (see Supplemental Experimental Procedures). Forty-three total properties were assessed. These occurrences were optionally scaled and used to calculate a second Sorensen coefficient which was given a weighting factor of 66.7. The two coefficients (topological torsions and general properties) were combined to given a total similarity score with 0 indicating "identical" molecules in this system and 100 indicating maximal dissimilarity. All characterization of molecules was done using in house software programs written in C.

X-ray Crystalllography

An N-terminal construct of human Hsp90α, residues 1–232, was used. Two- to threefold molar excess of compound (as a 100 mM DMSO stock) was added to 150 μM protein solution. Crystals were grown in 0.2 M $MgCl_2$, 0.1 M Bis-Tris (pH 6.5), and 20% PEG 3350 and were cryo-protected by adding 25% ethylene glycol to the mother liquor and passing the crystal through the solution immediately before flash freezing it in liquid nitrogen. The crystals were irregular shaped and measured approximately 300 × 200 × 100 μm and grew up over approximately 2 days. A Rigaku FR-E+ SuperBright, rotating anode, was used for data collection. Diffraction ambient temp was 113.15°C. Summary data are shown below. The coordinates and structure factor file will be deposited prior to publication.

Space Group: I222

Unit cell (Å): a = 66.773, b = 90.753, c = 99.116, a = 90°, b = 90°, g = 90°

Wavelength (Å): 1.5418
Resolution (Å): 36.45–1.90
No. of observations: 63297
No. of unique observations: 23,062
No. reflections, completeness (%): 21,887, 96
Redundancy: 2.74 (1.97–1.90 Å, 1.8)
Completeness (%): 95 (1.97–1.90 Å, 95)
I/σ(I): 10.8 (1.97–1.90 Å, 1.8)
R_sym: 0.084 (1.97–1.90 Å, 0.130)
R_cryst, R_free (5% data): 0.188, 0.235
Rms bonds (Å), rms angles (°): 0.009, 1.30
Residues in allowed region of Ramachandran plot (%): 100

Cell Proliferation and Client Protein Measurements

All cell experiments were performed as previously described (Barta et al., 2008) in 96-well assay plates. For proliferation assays, DNA from each treatment condition was quantified using CyQuant fluorescent dye from Invitrogen (Carlsbad, CA, USA). Levels of pS6/Hsp70 in A375 melanoma cells were measured concurrently using the Compartmental analysis algorithm from Cellomics (Pittsburg, PA). Individual cell nuclei were identified by Hoechst staining; cytoplasm staining intensities were then determined for a four pixel ring around the border of the identified nuclei. For each treatment condition, data were collected for a minimum of 250 objects, and the average staining intensity for each antibody was determined. For determining Her2/pERK in AU565 cells, data were collected for 500 individual objects per treatment condition, pERK intensity was determined for the nuclei area, and Her2 intensity was determined for a circular area encompassing both the nuclei and an additional four pixels into the cytoplasm.

Medicinal Chemistry

Methotrexate analogs **6** and **7** were synthesized as previously described (Hanson et al., 2006). The syntheses of benzamide compounds **14** and **15**, as well as SNX-2112 and SNX-5422, have also been reported (Huang et al., 2009).

Pharmacokinetics

In life work was conducted at Calvert Laboratories (Olyphant, PA). Female Sprague-Dawley rats were 6–7 weeks old and weighed 130–265 g. Single doses of SNX-5422 mesylate were administered by oral gavage to three groups of nine animals, at 10, 20, and 30 mg/kg. Blood samples were collected from three rats at each time point: 0.5, 1, 2, 4, 6, 8, 12, and 24 hr after dosing. Whole blood was collected from the retro-orbital sinus into chilled tubes containing sodium heparin, and the blood was converted to plasma in a refrigerated centrifuge. The samples were stored frozen until LC-MS/MS analysis.

The concentrations of SNX-5422 and SNX-2112 in rat plasma were determined by LC-MS/MS following protein precipitation with acetonitrile. The calibration curve ranges were 1.40–5250 and 1.60–6000 ng/ml for SNX-5422 and SNX-2112, respectively. The LC-MS/MS system consisted of a Shimadzu Prominence HPLC (Shimadzu, Columbia, MD) coupled to a hybrid triple quadrupole/linear ion trap mass spectrometer with a Turbospray source (QTRAP, Applied Biosystems, Foster City, CA). The samples were injected onto a Synergy Hydro-RP column, 2.0 × 30 mm, 4 μm (Phenomenex,

Torrance, CA), and the analytes and internal standard were eluted at a flow rate of 0.45 ml/min using a water-methanol gradient in the presence of 0.08–0.1% formic acid and 4 mM ammonium formate. The ESI mass spectrometer was operated in positive ion mode, using multiple reaction monitoring.

Mouse Xenografts

In life studies were performed at MIR (Michigan). SNX-5422 was suspended in a 1% CMC (carboxlymethylcellulose) / 5% Tween 80 solution (pH 6.5). Trastuzumab was obtained from OTN as a dry, white lyophilized powder and was stored in the dark at room temperature prior to being dissolved in sterile water to give a pH 7.7 solution. Female athymic nu/nu mice were obtained from Charles River. They were 7 weeks old on day 1 of the experiment. The animals were fed irradiated Rodent Diet 5053 (LabDiet) and water ad libitum. Mice were housed in static cages with Bed-O'Cobs bedding inside Biobubble Clean Rooms that provide H.E.P.A filtered air into the bubble environment at 100 complete air changes per hour. All treatments, body weight determinations, and tumor measurements were carried out in the bubble environment. The environment was controlled to a temperature range of 23° ± 2°C and a humidity range of 30%–70%.

Test animals were implanted subcutaneously on day 0 with 30–60 mg BT-474 tumor fragments using a 12 gauge trocar needle. All animals were observed for clinical signs at least once daily. Animals with tumors in excess of 1 g or with ulcerated tumors were euthanized, as were those found in obvious distress or in a moribund condition. All procedures carried out in this experiment were conducted in compliance with all the laws, regulations, and guidelines of the National Institutes of Health (NIH) and with the approval of MIR's Animal Care and Use Committee. Treatments began on day 53, when the mean estimated tumor mass for all groups in the experiment was 192 mg (range, 179–207 mg). All animals weighed >19.5 g at the initiation of therapy. Mean group body weights at first treatment were well matched (range, 22.7–24.2 g). All animals were dosed according to individual body weight on the day of treatment as indicated in the main text and Figure 5. Tumor measurements were recorded twice weekly. Tumor burden (mg) was estimated from caliper measurements by the formula for the volume of a prolate ellipsoid assuming unit density as: tumor burden (mg) = (L × W2)/2, where L and W are the respective orthogonal tumor length and width measurements (mm).

ACCESSION NUMBERS

Coordinates for the HSP90-SNX1321 crystal structure have been deposited in the RCSB protein data bank with accession code 3MNR.

SUPPLEMENTAL INFORMATION

Supplemental Information includes Supplemental Experimental Procedures and can be found with this article online at doi:10.1016/j.chembiol.2010.04.015.

ACKNOWLEDGMENTS

All authors are former employees of Serenex Inc. and may benefit financially if SNX-5422 progresses to additional clinical trials. We thank the following individuals and groups: Allison Cromwell, Michael Hast, and Tim Wadkins for assistance with proteome screening efforts; Klass Hardemann for resin preparation; David Blake and Carl Allen for research informatics support; Active Sight (San Diego, CA) for crystallography work; and Jon-Paul Strachan for synthetic efforts.

Received: September 30, 2009
Revised: March 16, 2010
Accepted: April 14, 2010
Published: July 29, 2010

REFERENCES

Banerji, U. (2009). Heat shock protein 90 as a drug target: some like it hot. Clin. Cancer Res. *15*, 9–14.

Bantscheff, M., Eberhard, D., Abraham, Y., Bastuck, S., Boesche, M., Hobson, S., Mathieson, T., Perrin, J., Raida, M., Rau, C., et al. (2007). Quantitative chemical proteomics reveals mechanisms of action of clinical ABL kinase inhibitors. Nat. Biotechnol. *25*, 1035–1044.

Barta, T.E., Veal, J.M., Rice, J.W., Partridge, J.M., Fadden, R.P., Ma, W., Jenks, M., Geng, L., Hanson, G.J., Huang, K.H., et al. (2008). Discovery of benzamide tetrahydro-4H-carbazol-4-ones as novel small molecule inhibitors of Hsp90. Bioorg. Med. Chem. Lett. *18*, 3517–3521.

Brough, P.A., Aherne, W., Barril, X., Borgognoni, J., Boxall, K., Cansfield, J.E., Cheung, K.M., Collins, I., Davies, N.G., Drysdale, M.J., et al. (2008). 4,5-diarylisoxazole Hsp90 chaperone inhibitors: potential therapeutic agents for the treatment of cancer. J. Med. Chem. *51*, 196–218.

Calderwood, S.K., Khaleque, M.A., Sawyer, D.B., and Ciocca, D.R. (2006). Heat shock proteins in cancer: chaperones of tumorigenesis. Trends Biochem. Sci. *31*, 164–172.

Carrez, C., Fassy, F., Mailliet, P. (2006). PCT Int. Appl. WO2006075095.

Chandarlapaty, S., Sawai, A., Ye, Q., Scott, A., Silinski, M., Huang, K., Fadden, P., Partdrige, J., Hall, S., Steed, P., et al. (2008). SNX2112, a synthetic heat shock protein 90 inhibitor, has potent antitumor activity against HER kinase-dependent cancers. Clin. Cancer Res. *14*, 240–248.

Chiosis, G., and Tao, H. (2006). Purine-scaffold Hsp90 inhibitors. IDrugs *9*, 778–782.

Chiosis, G., Vilenchik, M., Kim, J., and Solit, D. (2004). Hsp90: the vulnerable chaperone. Drug Discov. Today *9*, 881–888.

Duncan, J.S., Gyenis, L., Lenehan, J., Bretner, M., Graves, L.M., Haystead, T.A., and Litchfield, D.W. (2008). An unbiased evaluation of CK2 inhibitors by chemoproteomics: characterization of inhibitor effects on CK2 and identification of novel inhibitor targets. Mol. Cell. Proteomics *7*, 1077–1088.

Dymock, B.W., Barril, X., Brough, P.A., Cansfield, J.E., Massey, A., McDonald, E., Hubbard, R.E., Surgenor, A., Roughley, S.D., Webb, P., et al. (2005). Novel, potent small-molecule inhibitors of the molecular chaperone Hsp90 discovered through structure-based design. J. Med. Chem. *48*, 4212–4215.

Eggenweiler, H., Wolf, M. November 2006. PCT Int. Appl. WO2006125531.

Eggenweiler, H., Wolf, M., Buchstaller, H. November 2006. PCT Int. Appl. WO2006122631.

Esser, L., Wang, C.R., Hosaka, M., Smagula, C.S., Südhof, T.C., and Deisenhofer, J. (1998). Synapsin I is structurally similar to ATP-utilizing enzymes. EMBO J. *17*, 977–984.

Finn, R.D., Tate, J., Mistry, J., Coggill, P.C., Sammut, S.J., Hotz, H.R., Ceric, G., Forslund, K., Eddy, S.R., Sonnhammer, E.L., and Bateman, A. (2008). The Pfam protein families database. Nucleic Acids Res. *36*, D281–D288.

GAO-07-49. (2006). New Drug Development: Science, Business, Regulatory, and Intellectual Property Issues Cited as Hampering Drug Development Efforts, United States Government Accountability Office Report to Congressional Requesters.

Gharahdaghi, F., Weinberg, C.R., Meagher, D.A., Imai, B.S., and Mische, S.M. (1999). Mass spectrometric identification of proteins from silver-stained polyacrylamide gel: a method for the removal of silver ions to enhance sensitivity. Electrophoresis *20*, 601–605.

Gooljarsingh, L.T., Fernandes, C., Yan, K., Zhang, H., Grooms, M., Johanson, K., Sinnamon, R.H., Kirkpatrick, R.B., Kerrigan, J., Lewis, T., et al. (2006). A biochemical rationale for the anticancer effects of Hsp90 inhibitors: slow, tight binding inhibition by geldanamycin and its analogues. Proc. Natl. Acad. Sci. USA *103*, 7625–7630.

Graves, P.R., Kwiek, J.J., Fadden, P., Ray, R., Hardeman, K., Coley, A.M., Foley, M., and Haystead, T.A. (2002). Discovery of novel targets of quinoline drugs in the human purine binding proteome. Mol. Pharmacol. *62*, 1364–1372.

Guillerm, G., Muzard, M., Glapski, C., Pilard, S., and De Clercq, E. (2006). Inactivation of S-adenosyl-L-homocysteine hydrolase by 6′-cyano-5′, 6′-didehydro-6′-deoxyhomoadenosine and 6′-chloro-6′-cyano-5′,6′-didehydro-6′-deoxyhomoadenosine. Antiviral and cytotoxic effects. J. Med. Chem. *49*, 1223–1226.

Hanson, G.J., Barta, T.E., Veal, J.M., Ware, R.W. February 2006. PCT Int. Appl. WO2006014706.

Hardeman, K., Hall, S.E., Ware, R.W., Hinckley, L.A., Jenks, M.G. August 2004. PCT Int. Appl. WO2004065566.

Harwood, H.J. (2004). Acetyl-CoA carboxylase inhibition for the treatment of metabolic syndrome. Curr. Opin. Investig. Drugs *5*, 283–289.

Haystead, T.A. (2006). The purinome, a complex mix of drug and toxicity targets. Curr. Top. Med. Chem. *6*, 1117–1127.

Huang, K.H., Veal, J.M., Fadden, R.P., Rice, J.W., Eaves, J., Strachan, J.P., Barabasz, A.F., Foley, B.E., Barta, T.E., Ma, W., et al. (2009). Discovery of novel 2-aminobenzamide inhibitors of heat shock protein 90 as potent, selective and orally active antitumor agents. J. Med. Chem. *52*, 4288–4305.

Immormino, R.M., Kang, Y., Chiosis, G., and Gewirth, D.T. (2006). Structural and quantum chemical studies of 8-aryl-sulfanyl adenine class Hsp90 inhibitors. J. Med. Chem. *49*, 4953–4960.

Janin, Y.L. (2005). Heat shock protein 90 inhibitors. A text book example of medicinal chemistry? J. Med. Chem. *48*, 7503–7512.

Kasibhatla, S.R., Hong, K., Biamonte, M.A., Busch, D.J., Karjian, P.L., Sensintaffar, J.L., Kamal, A., Lough, R.E., Brekken, J., Lundgren, K., et al. (2007). Rationally designed high-affinity 2-amino-6-halopurine heat shock protein 90 inhibitors that exhibit potent antitumor activity. J. Med. Chem. *50*, 2767–2778.

Machajewski, T.D., Zhenhai, G., Levine, B.H., William, A., Bellamacina, C., Costales, A., Doughan, B.M., Fong, S., Hendrickson, T., Lin, X., et al. October 2006). PCT Int. Appl. WO2006113498.

Neckers, L. (2007). Heat shock protein 90: the cancer chaperone. J. Biosci. *32*, 517–530.

Obermann, W.M., Sondermann, H., Russo, A.A., Pavletich, N.P., and Hartl, F.U. (1998). In vivo function of Hsp90 is dependent on ATP binding and ATP hydrolysis. J. Cell Biol. *143*, 901–910.

Panaretou, B., Prodromou, C., Roe, S.M., O'Brien, R., Ladbury, J.E., Piper, P.W., and Pearl, L.H. (1998). ATP binding and hydrolysis are essential to the function of the Hsp90 molecular chaperone in vivo. EMBO J. *17*, 4829–4836.

Patricelli, M.P., Szardenings, A.K., Liyanage, M., Nomanbhoy, T.K., Wu, M., Weissig, H., Aban, A., Chun, D., Tanner, S., and Kozarich, J.W. (2007). Functional interrogation of the kinome using nucleotide acyl phosphates. Biochemistry *46*, 350–358.

Pearl, L.H., and Prodromou, C. (2006). Structure and mechanism of the Hsp90 molecular chaperone machinery. Annu. Rev. Biochem. *75*, 271–294.

Powers, M.V., and Workman, P. (2007). Inhibitors of the heat shock response: biology and pharmacology. FEBS Lett. *581*, 3758–3769.

Pratt, W.B., and Toft, D.O. (2003). Regulation of signaling protein function and trafficking by the hsp90/hsp70-based chaperone machinery. Exp. Biol. Med. (Maywood) *228*, 111–133.

Prodromou, C., Roe, S.M., O'Brien, R., Ladbury, J.E., Piper, P.W., and Pearl, L.H. (1997). Identification and structural characterization of the ATP/ADP-binding site in the Hsp90 molecular chaperone. Cell *90*, 65–75.

Roe, S.M., Prodromou, C., O'Brien, R., Ladbury, J.E., Piper, P.W., and Pearl, L.H. (1999). Structural basis for inhibition of the Hsp90 molecular chaperone by the antitumor antibiotics radicicol and geldanamycin. J. Med. Chem. *42*, 260–266.

Rosenfeld, J., Capdevielle, J., Guillemot, J.C., and Ferrara, P. (1992). In-gel digestion of proteins for internal sequence analysis after one- or two-dimensional gel electrophoresis. Anal. Biochem. *203*, 173–179.

Schulte, T.W., Akinaga, S., Soga, S., Sullivan, W., Stensgard, B., Toft, D., and Neckers, L.M. (1998). Antibiotic radicicol binds to the N-terminal domain of Hsp90 and shares important biologic activities with geldanamycin. Cell Stress Chaperones *3*, 100–108.

Sharma, S.V., Agatsuma, T., and Nakano, H. (1998). Targeting of the protein chaperone, HSP90, by the transformation suppressing agent, radicicol. Oncogene *16*, 2639–2645.

Solit, D.B., and Chiosis, G. (2008). Development and application of Hsp90 inhibitors. Drug Discov. Today *13*, 38–43.

Stebbins, C.E., Russo, A.A., Schneider, C., Rosen, N., Hartl, F.U., and Pavletich, N.P. (1997). Crystal structure of an Hsp90-geldanamycin complex: targeting of a protein chaperone by an antitumor agent. Cell *89*, 239–250.

UniProt Consortium. (2008). The universal protein resource (UniProt). Nucleic Acids Res. *36*, D190–D195.

Vilenchik, M., Solit, D., Basso, A., Huezo, H., Lucas, B., He, H., Rosen, N., Spampinato, C., Modrich, P., and Chiosis, G. (2004). Targeting wide-range oncogenic transformation via PU24FCl, a specific inhibitor of tumor Hsp90. Chem. Biol. *11*, 787–797.

Vogel, C.L., Cobleigh, M.A., Tripathy, D., Gutheil, J.C., Harris, L.N., Fehrenbacher, L., Slamon, D.J., Murphy, M., Novotny, W.F., Burchmore, M., et al. (2002). Efficacy and safety of trastuzumab as a single agent in first-line treatment of HER2-overexpressing metastatic breast cancer. J. Clin. Oncol. *20*, 719–726.

Sørensen, T. (1948). A method of establishing groups of equal amplitude in plant sociology based on similarity of species and its application to analyses of the vegetation on Danish commons. Biologiske Skrifter / Kongelige Danske Videnskabernes Selskab *5*, 1–34.

Whitesell, L., and Lindquist, S.L. (2005). HSP90 and the chaperoning of cancer. Nat. Rev. Cancer *5*, 761–772.

Whitesell, L., Mimnaugh, E.G., De Costa, B., Myers, C.E., and Neckers, L.M. (1994). Inhibition of heat shock protein HSP90-pp60v-src heteroprotein complex formation by benzoquinone ansamycins: essential role for stress proteins in oncogenic transformation. Proc. Natl. Acad. Sci. USA *91*, 8324–8328.

Wright, L., Barril, X., Dymock, B., Sheridan, L., Surgenor, A., Beswick, M., Drysdale, M., Collier, A., Massey, A., Davies, N., et al. (2004). Structure-activity relationships in purine-based inhibitor binding to HSP90 isoforms. Chem. Biol. *11*, 775–785.

